Journal of Thermal Analysis and Calorimetry, Vol. 79 (2005) 537–543

THE FORMATION AND PRODUCTION OF NANO AND MICRO PARTICLES ON CLAYS UNDER ENVIRONMENTAL-LIKE CONDITIONS

J. Kónya[1*], *N. M. Nagy*[1] *and M. Földvári*[2]

[1]Isotope Laboratory, University of Debrecen, Debrecen 4010, Hungary
[2]Hungarian Geological Survey, Budapest, Hungary

Metal ions are adsorbed in the interlayer space and on the edges of clay minerals, leading to the uniform distribution of metal ions on atomic scale. However, additional processes can be resulted in the formation of nano and micro particles in the interlayer space as well as on the outer surfaces. The formation of nano and micro particles on clay minerals under environmental conditions are discussed here in metal ions (manganese, lead, zinc, and silver ions)/bentonite systems. Two-dimensional nano layer is formed in the interlayer space by the oxidation of manganese ions under atmospheric conditions. Three-dimensional particles are formed on the surfaces initiating by the metal ion adsorption on the deprotonated edge sites. The formation of micro particles on the surface can also be followed by the redox reaction of metal ions.

Keywords: *bentonite, lead, manganese, micro particles, nano particles, silver, zinc*

Introduction

Clay minerals are important constituents of the natural environment. By their interfacial reactions they play an important role in several fields, for example in the nutrient cycle of soils, in the environmental protection, or even in the synthetic chemical industry. One of the interfacial reactions of clay minerals is the adsorption and cation exchange of metal ions.

Metal ions can be adsorbed in the interlayer space of some clay minerals (e.g. montmorillonite) and on the pH-dependent charges, silanol and aluminol sites, on the edges of clay minerals. The ratio of the two ways of cation adsorption depends on pH, but about 80–90% of the cation adsorption comes from the neutralization of the layer charges, so this way of cation adsorption is determining [1].

The nature of the adsorption is different: in the interlayer space electrostatic forces are important; the ratio of charge and the cation size determines the adsorption ability. Cations in the interlayer space have their hydrate sphere. This process is the so-called outer-sphere complexation. On the edge charges the chemical properties of the metal ions are significant. The cations adsorb on the edge charges by oxygen-cation bonds, without hydrate sphere. This process is called inner-sphere complexation [2, 3].

Both ways of cation adsorption primarily leads to the uniform distribution of metal ions on atomic scale. However, additional processes can be resulted in the formation of nano and micro particles in the interlayer space as well as on the outer surfaces. Nano and micro particles on clays have been produced by different chemical procedures [e.g. 4], but they can be formed under environmental conditions. In this paper the formation of nano and micro particles on clay minerals under environmental conditions are discussed in metal ions (manganese, lead, zinc, and silver ions)/bentonite systems. A really natural micro particle on clay sediment is also shown.

Manganese ion can take part as a component of the pillaring agent [5–8] in the production of pillared clays. Slow hydrolysis of hydrated Mn(II) in Mn(II)-montmorillonite was detectable with ESR studies, and the formation of $[Mn(OH)(H_2O)_5]^+$ was proposed [9]. Andreux and Stocky [10] used Mn(II)-montmorillonite and manganese oxide (within other catalysts) in the polymerisation of catechol in the presence of triglycine.

Lead-clay interactions have received the most attention to date. Lead sorption increases with increasing pH and significantly increases after the precipitation of lead hydroxide [11–14]. Other studies looked at sites where lead resided in the clay minerals and the mechanisms that put it there. Shen *et al*. [13] studied the sorption of lead ion by Na-montmorillonite using Fourier transform infrared spectroscopy and X-ray diffraction. They observed that the sodium-lead exchange increased the basal spacing of the montmorillonite and increased the intensities of the OH bending bands. They explained the adsorbed lead quantity by the chemical speciation of lead.

* Author for correspondence: konya@tigris.klte.hu

1388–6150/$20.00

Akadémiai Kiadó, Budapest, Hungary
Springer, Dordrecht, The Netherlands

Strawn and Sparks [2] used X-ray absorption fine structure (XAFS) spectroscopy to study the adsorption of lead ion by montmorillonite and found there were two different lead adsorption mechanisms. These mechanisms were controlled by ionic strength. The low ionic strength mechanism is pH independent and is consistent with an outer-sphere complexation. The high ionic strength mechanism is pH dependent and suggests inner-sphere complexation where lead forms covalent bonds.

Other studies have examined the competition among different heavy metal ions (copper, zinc, cadmium, lead, etc.) for exchange sites [e.g. 15–18]. More detailed studies evaluated lead adsorption by Langmuir or Freundlich isotherms, and the competition of other cations by competitive Langmuir isotherms.

In case of clay minerals the thermal analysis is mainly used for the study of clay-organic composites [e.g. 19, 20], but this method, together with other analytical techniques, can give very useful information on the interfacial processes on different cation exchanged clays as well.

Experimental

Manganese, lead-, zinc- and silver-bentonite were produced from calcium-bentonite (Istenmezeje, Hungary). The mineral composition was determined by X-ray diffraction and thermoanalytical studies and found as follows: 91% montmorillonite, 4% kaolinite, 5% calcite. Cation-exchange capacity of 1.04 mmol g^{-1} for monovalent cations was determined by the ammonium acetate method [21]. Manganese-, lead-, zinc- and silver-montmorillonite were produced from calcium-montmorillonite by several ion exchange procedures [22–27]. The conditions are summarized in Table 1. The free cations were removed by washing with double distilled water ten times (metal traces were not observed after sixth wash).

The manganese, lead, zinc and silver contents of the cation-exchange bentonites were measured by X-ray fluorescence analysis.

The cation exchanged bentonites were studied by different techniques, the instruments and operating parameters are listed in Table 2 [26].

Natural clay sediment containing calcium-montmorillonite was collected from Lake Prod (next to Road No. 35 in Eastern Hungary). The average depth of the lake is 1.2 m. Three randomly selected samples from the upper 30 cm of sediment were analyzed for total lead by microwave digestion and ICP-OES, and the total lead concentrations were 22.7, 36.3 and 35.1 mg kg^{-1}.

Results and discussions

Manganese-bentonite

Manganese ion, for the first site, shows no special properties during the ion exchange on bentonite that is manganese(II) ions are adsorbed in the interlayer space of montmorillonite [22, 23, 28]. However, manganese-bentonite is kept in room atmosphere for a long time (1–2 years), the color and other chemical and physical properties change. The color of the old manganese-bentonite is darker than the fresh sample and similar to the color of manganese-dioxide (Fig. 1). The brown color refers to the oxidation of manganese in bentonite.

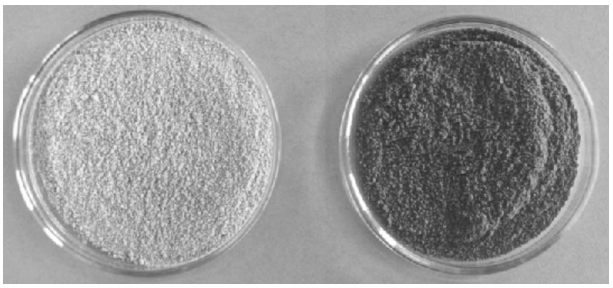

Fig. 1 Photos of fresh and old manganese-bentonites

Similarly, the thermoanalytical studies (Fig. 2) also show the oxidation of manganese(II) in bentonite. In Fig. 2 TG, DTG and DTA curves of fresh and old manganese-bentonites are shown. The thermoanalytical curves of clays can usually be divided into two regions: (1) the region of the dehydration of clay (below 200–250°C) [20], (2) the endothermic dehydroxylation of the clay (above 500°C) which is followed by a small exothermic peak of the recrystallization. Both regions

Table 1 Experimental conditions of the productions of manganese-, lead-, zinc- and silver-bentonites

	Mass of Ca-montmorillonite/g	Solution	pH	Number of treatments	Drying temperature/°C
Mn-bentonite	20	200 cm^3 0.01 mol dm^{-3} $Mn(ClO_4)_2$	6.5	7	25
Pb-bentonite	50	100 cm^3 0.1 mol dm^{-3} $Pb(ClO_4)_2$	2.9	7	25
Zn-bentonite	50	200 cm^3 0.1 mol dm^{-3} $Zn(ClO_4)_2$	5.5	7	25
Ag-bentonite	10	25 cm^3 0.03 mol dm^{-3} $AgClO_4$	3.9	7	25

Table 2 Instruments and operating parameter

X-ray fluorescence elementary composition and metal ions of cation exchanged clay	RONTEC EDR 288 energy dispersive X-ray spectrometer
Thermoanalysis clay structure	Derivatograph-PC, a computer-controlled simultaneous TG, DTG, DTA apparatus. 10°C min^{-1} heating rate, air atmosphere, ceramic crucible, mass sample about 100 mg, reference material Al_2O_3
XRD clay structure	Philips PW 1710 Diffractometer with graphite monochromator, CuK_α radiation (30 mA and 40 kV), scanning rate of 2° 2Θ min^{-1}
pH measurement suspensions and liquid phase after filtration	Metrohm 654 pH meter with 6.0220.100 electrode
Redox potential measurement	Metrohm 654 pH meter, reference electrode saturated calomel
ICP total Pb in sediment	Milestone MLS-1200 MEGA microwave oven and Spectroflame ICP-OES (inductively coupled plasma – optical emission spectrometer) microwave digestion: 300 mg dry sediment with 1 cm^3 concentrated H_2O_2 and 4 cm^3 concentrated HNO_3 in a teflon bomb
SEM physical structure	Amray –1830 Scanning Electron Microscope HITACHI S-570 I Scanning Electron Microscope. Morphology of the sample can be seen by back scattered electrons. Metal ion maps (e.g. lead map in Fig. 5) can be made by characteristic X-ray photons. Metal ion (e.g. lead) concentration is proportional to the density of the light spots
AFM physical structure	Nanoscope III Atomic Force Microscope
XPS Mn and Pb speciation	ATOMKI ESA-31 Spectrometer with non monochromated AlK_α radiation, energy calibration with polycrystalline Cu and Ag samples, correction for charging (energy shift of ca. 8.4 eV) was made. Referencing C 1s line with Eb=285 eV

can be observed in Fig. 2, namely the elimination of interlayer water (at 120°C) and the endothermic dehydroxylation above 500°C. In addition the elimination of water coordinated to manganese(II) ion (at 260°C) are well distinguished in the DTA and DTG curves [23]. This peak of the dehydration of manganese(II) is more intense in DTG curve for the fresh manganese-bentonite that for the old manganese-bentonite where this peak cannot be observed practically. The exothermal oxidation of manganese(II) to manganese(IV) is also more significant in DTA curve for the fresh sample where the endothermic dehydroxylation of the bentonite at high temperatures is compensated by the exothermic oxidation of manganese(II) to manganese(IV). This compensation is not observed on the DTA curve for the old manganese-bentonite where the major part of manganese has been oxidized previously, not during the thermal analysis.

ESCA studies show similar results: the oxidation state of manganese is II in the fresh sample; a more oxidized state is present in the old sample. Redox potential is more positive in the case of the old manganese-bentonite, too. It means more oxidized species for manganese in the old sample.

The oxidation of manganese occurs in the difference of adsorption and catalytic properties. For example valine amino acid does not adsorb on fresh manganese-bentonite, while it is adsorbed on old manganese-bentonite [27]. The old manganese bentonite catalysis the destruction of hydrogen peroxide, fresh manganese-bentonite, however, has no catalytic effect on the destruction of hydrogen-peroxide.

At the same time the concentration of manganese ions remains the same. The basal spacing of montmorillonite (001) determined by X-ray diffraction are very similar for the new (1.51 nm) and old (1.48 nm) samples. The distribution of manganese determined by scanning electron microscopy is also uniform in the old samples, similarly to fresh samples (Fig. 3).

As a conclusion we can say that manganese(II) ions adsorbed in the interlayer space of montmorillonite by cation exchange reactions are spontaneously oxidized to manganese(IV) under atmospheric conditions. Consequently, the properties relating to the oxidation state of manganese are different for the fresh and old manganese-bentonite samples. The concentrations, distribution of manganese as well as the structure of bentonite, however, do not change. The increase of the positive charge of manganese demands the neutralization of the extra positive charge by oxide or hydroxide ions originated from the atmosphere, because the negative layer charge of the clay minerals is constant.

These results show that a two-dimensional nano layer is formed in the interlayer space where manganese ion is bonded to the clay layers by two positive charges and to oxides or hydroxides by the other two positive charges. The presence of a 2D layer of manganese in the interlayer space of montmorillonite is obvious because the montmorillonite has layered structure and manganese ions introduce into the interlayer space by cation exchange. For this reason the distribution of manganese ions is uniform (as seen by scanning electron microscope, too) and it does not change under oxidation.

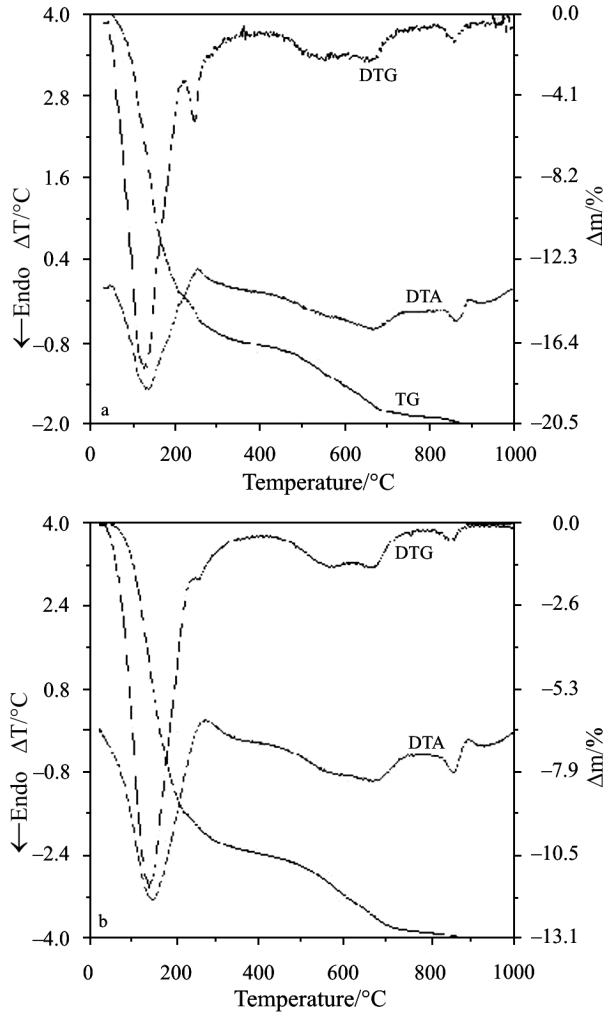

Fig. 2 Thermoanalytical curves of a – fresh and b – old Mn-bentonites

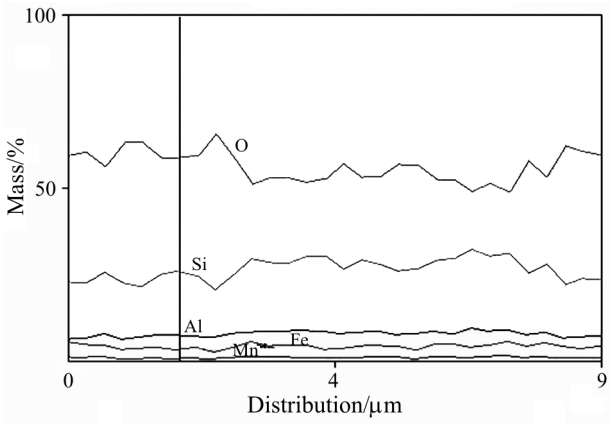

Fig. 3 The concentration profile of different elements of fresh manganese-bentonite

Lead-bentonite

The scanning electron microscopic picture of lead-bentonite shows that the distribution of lead is fairly even on the major part of the surface. However, there are places where the concentration of lead is higher than the mean surface concentration (cca. 10%) (Fig. 4). Since SEM's horizontal and vertical resolutions are approximately 1 μm, the uncertainty of both the position and the diameter of these spots is also about 1 μm. These enrichments are relatively weakly adsorbed on the surface of bentonite because when a freshly cleaved mica surface is immersed into the suspension containing bentonite and lead ions they easily adsorbed on the surface of mica as seen on SEM (Fig. 5) or AFM pictures (Fig. 6). The diameter of them is from hundred nanometers to micrometer. The presence of lead enrichments with smaller diameter can also be possible but they are more strongly adsorbed and cannot be desorbed from the surface by this very simple method. Similar lead enrichments were found on a natural clay sediment of a lake in Hungary (Fig. 7).

The results show [24, 26, 29] that lead ions are adsorbed on bentonite by two processes: by cation exchange in the interlayer space of montmorillonite (outer-sphere complexation) and by adsorption on the edge sites (inner-sphere complexation). Cation exchange leads to the even distribution of the ions, while the adsorption on the edge sites can act as the initial of a heterogeneous nucleation on particle surface followed by a crystal growth. The nano and micro particles (lead enrichments) seen by SEM and AFM can likely be formed on these nuclei. The production of

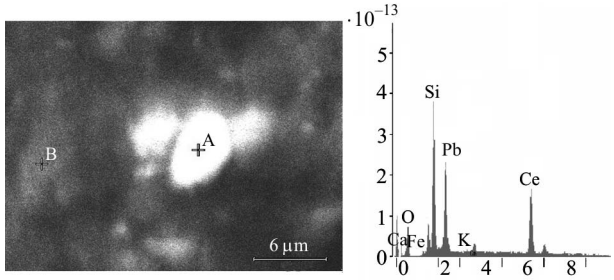

Fig. 4 Left side – scanning electron microscopic picture of lead bentonite. Right side – the elementary analysis of the white spot between points A and B

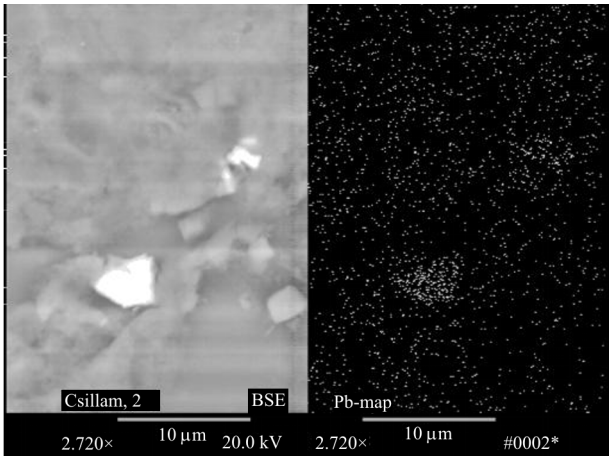

Fig. 5 Scanning electron microscopic picture of freshly cleaved mica surfaces immersed into the suspension containing suspension of lead-bentonite. Left side – morphology of the sample made by back scattered electrons. Right side – lead map made by characteristic X-ray photons. Lead concentration is proportional to the density of the light spots

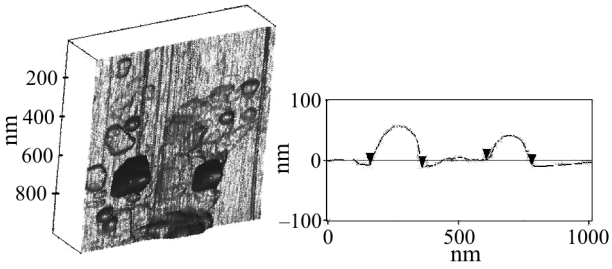

Fig. 6 Left side – atomic force microscopic picture of a freshed cleaved mica immersed into the suspension of lead-bentonite. Right side – the diameter of the black spots on the left picture

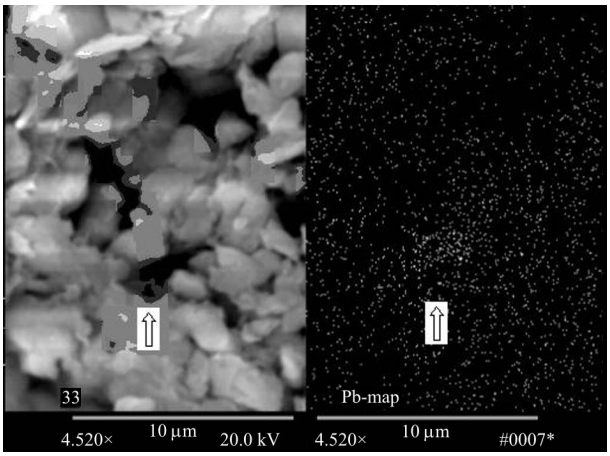

Fig. 7 Scanning electron microscopic picture of a natural clay sediment. Mean lead concentration is 36 mg kg^{-1}, lead map in the window. Left side – morphology of the sample made by back scattered electrons. Right side – lead map made by characteristic X-ray photons. Lead concentration is proportional to the density of the light spots

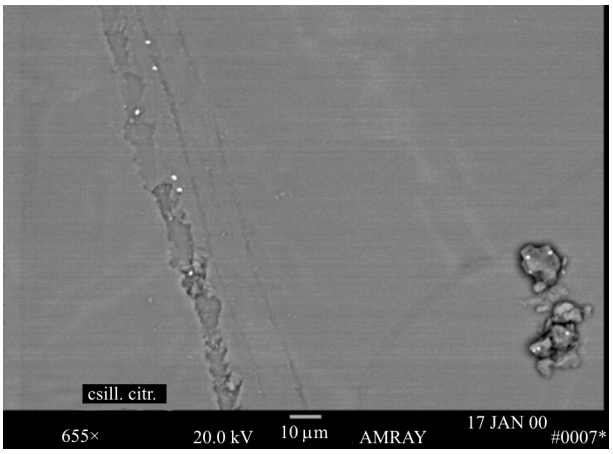

Fig. 8 Scanning electron microscopic picture of freshly cleaved mica surfaces immersed into the suspension containing suspension of lead-bentonite in the presence of citric acid. White spots are lead micro particles

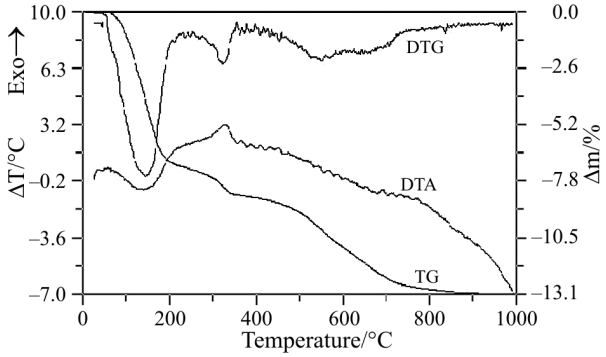

Fig. 9 Thermoanalytical curves of lead-bentonite

these particles is not expected from thermodynamic properties under conditions of the bulk solution (acidic pH) and cannot be observed in the absence of clay. On the basis of the solubility product of $Pb(OH)_2$ (L=6.8·10^{-13}) lead is present as Pb^{2+} at pH values of the experiments. The formation of lead enrichments requires the presence of the clay. In the presence of clay lead enrichments are formed even in solution containing a complex forming agent (citric acid) (Fig. 8).

The thermoanalytical curves of lead-bentonite are shown in Fig. 9.

The peaks at low temperatures are similar as usual for bentonites [23], but there is a new exothermic reaction in the range of 320–350°C which can be the reaction of the surface micro particles. At the same time TG curve shows the decrease of the mass. Similar thermoanalytical behavior has been evaluated by the presence of hydroxides (e.g. gibbsite). The presence of hydroxide is proved by the X-ray diffactograms where a peak characteristic to hydroxides.

Zinc-bentonite

In case of zinc-bentonite the adsorbed quantity of zinc ions after the cation exchange is about 1.4 times greater than the cation exchange capacity of bentonite [30, 31]. It shows that similar micro particles have to be observed in the case of zinc-bentonite (Fig. 10). These particles, however, are less remarkable than in case of lead-bentonite, the appearance of them can be proved by the statistical analysis of the distribution of the white spots on SEM pictures. They are adsorbed on the surface of bentonite more strongly than lead containing micro particles because they cannot be transferred to the surface of freshly cleaved mica.

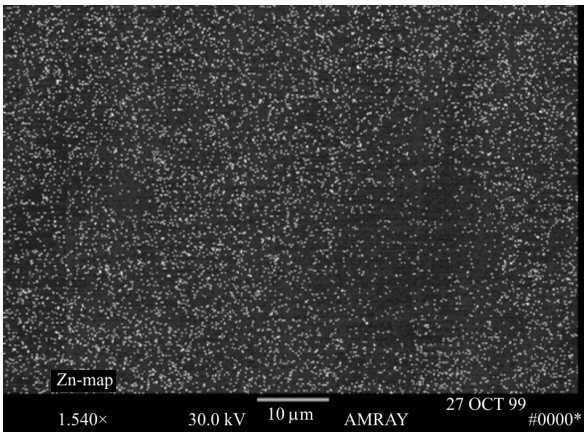

Fig. 10 Scanning electron microscopic picture of zinc-bentonite, Zn map on the basis of characteristic X-ray photons. Zinc concentration is proportional to the density of the light spots

The mechanism of the formation of the zinc enrichments can be similar to lead-bentonite. A part of zinc ion is exchanged by the cations in the interlayers (equivalent to cation exchange capacity). The excess amount of zinc ion is adsorbed on the deprotonated edge sites. Since the amount of edge sites is about 10–20% of cation exchange capacity [27] and the excess of the adsorbed amount of zinc ion is about 40%, heterogeneous nucleation must be supposed.

Silver-bentonite

In case of silver-bentonite similar silver micro particles can be observed as in the case of lead-bentonite (Fig. 11). In addition some silver enrichments were SEM studies show about 100% silver content. It shows that the reduction of silver(I) to metallic silver can also be taken place.

The thermoanalytical curves of silver-bentonite are shown in Fig. 12.

Figure 12 shows an exothermal reaction at 361°C. It refers to the oxidation of metallic silver. It is proved by the change of the color of silver-bentonite which is originally dark grey and becomes light after the heat treatment.

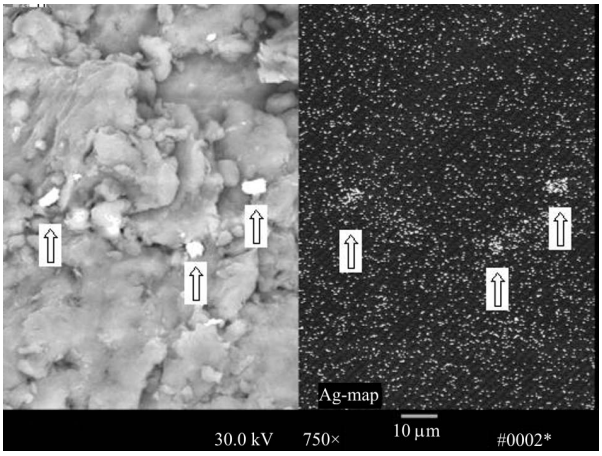

Fig. 11 Scanning electron microscopic picture of silver-bentonite. Left side – morphology of the sample made by back scattered electrons. Right side – lead map made by characteristic X-ray photons. Silver concentration is proportional to the density of the light spots. The arrows show spots with 100% silver concentration

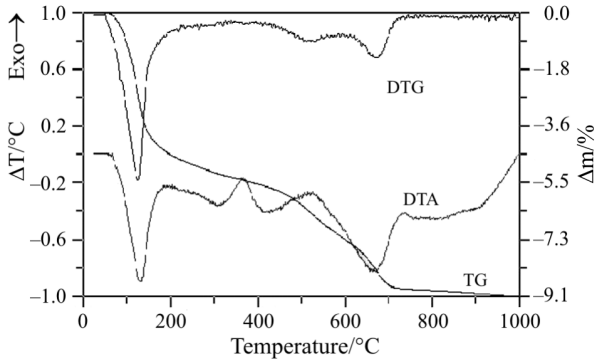

Fig. 12 Thermoanalytical curves of silver-bentonite

The redox conditions and the mechanism of metallic silver needs additional studies.

Conclusions

Beside the usual ion adsorption reactions, nano and micro particles can also be formed in the interlayer space as well as on the surface of clay minerals. These particles can be two- (2D) or three-dimensional (3D). Two-dimensional nano layer is formed in the interlayer space of montmorillonite by the spontaneous oxidation of manganese ions under atmospheric conditions. Three-dimensional particles are formed on the surfaces of clay minerals initiating by the metal ion (for example lead or zinc ions) adsorption on the deprotonated edge sites. The formation of micro particles on the surface can also be followed by the redox reaction of the metal ion (e.g. reduction of silver ion).

Acknowledgements

The authors thank Imre Beszeda, Erika Kálmán *et al*., Péter Kovács-Pálffy for their help. One of the authors (Nagy) thank the Ministry of Education for Széchenyi grant.

References

1 H. van Olphen, An Introduction to Clay Colloid Chemistry, Interscience, New York 1977.
2 D. G. Strawn and D. L. Sparks, J. Colloid Interface Sci., 216 (1999) 257.
3 M. E. Schrader, G. I. Loeb (Eds) Modern approaches to Wettability: Theory and applications. Plenum Publishing Corporation, New York 1992, p. 279.
4 S. Papp and I. Dékány, Colloid Polym. Sci., 281 (2003) 727.
5 K. Kawano, S. B. Madhu, M. Mizutamari and R. Nakata, J. Phys. Chem. Solids, 64 (2003) 77.
6 T. Mishra and K. Parida, J. Mater. Chem., 7 (1997) 147.
7 M. L. Cao, Y. F. Yu, J. Z. Yuang and M. H. Cao, J. Wuhan Univ. Technol., 17 (2002) 43.
8 L. M. Gandía, M. A. Vicente, P. Oelker, P. Grange and A. Gil, React. Kinet. Catal. Let., 64 (1998) 145.
9 P. Monsef-Mirzai and W. R. McWhinnie, Inorg. Chim. Acta, 73 (1983) 41.
10 F. G. Andreux and G. Stotzky, Sci. Total Environ., 117/118 (1992) 345.
11 O. Altin, O. H. Ozbelge and T. Dogu, J. Chem. Tech. Biotech., 74 (1999) 1131.
12 O. Altin, O. H. Ozbelge and T. Dogu, J. Chem. Tech. Biotech., 74 (1999) 1139.
13 S. Shen, W. T. Taylor, H. Bart and Sh-I. Tu, Commun. Soil Sci. Plant Anal., 30 (1999) 2711.
14 F. Barbier, G. Duc and M. Petit-Ramel, Colloids Surf., 166 (2000) 153.
15 C. Breen, C. M. Bejarano-Bravo, L. Madrid, G. Thompson and B. E. Mann, Colloids Surf., 155 (1999) 211.
16 S. Kaoser, S. Barrington and N. Elektrowicz, Soil Sedim. Contam., 9 (2000) 503.
17 M. T. Prado, Comm. Soil Sci. Plant Anal., 31 (2000) 31.
18 Q. X. Wu, W. H. Hendershot, W. D. Marshall and Y. Ge, Comm. Soil Sci. Plant Anal., 31 (2000) 1129.
19 M. Kubranová, E. Jóna, E. Rudinská, K. Nemceková, D. Ondrusová and M. Pajtásová, J. Therm. Anal. Cal., 74 (2003) 251.
20 Z. Yermiyahu, A. Landau, A. Zaban, I. Lapides and S. Yariv, J. Therm. Anal. Cal., 72 (2003) 431.
21 L. A. Richards, Diagnosis and Improvement of Saline and Alkaline Soils, US Dept. Agr. Handbook, Vol. 60 1957.
22 N. M. Nagy, J. Kónya and T. Budai, Colloids Surf., 138 (1998) 81.
23 M. Földvári, P. Kovács-Pálffy, N. M. Nagy and J. Kónya, J. Thermal Anal., 53 (1998) 547.
24 N. M. Nagy, J. Kónya, M. Beszeda, I. Beszeda, E. Kálmán, Zs. Keresztes and K. Papp, Proc. Colloid Polym. Sci., 117 (2001) 117.
25 N. M. Nagy, M. A. Jakab, J. Kónya and S. Antus, Appl. Clay Sci., 21 (2002) 213.
26 N. M. Nagy, J. Kónya, M. Beszeda, I. Beszeda, E. Kálmán, Zs. Keresztes, K. Papp and I. Cserny, J. Colloid Interface Sci., 263 (2003) 13.
27 N. M. Nagy and J. Kónya, Appl. Clay Sci., 25 (2004) 57.
28 N. M. Nagy and J. Kónya, Reactive Polymers, l7 (1992) 9.
29 N. M. Nagy, J. Kónya and I. Kónya, Colloids Surf., 137 (1998) 243.
30 J. Kónya, N. M. Nagy and K. Szabó, Reactive Polymers, 7 (l988) 203.
31 N. M. Nagy and J. Kónya, Colloids Surf., 32 (l988) 223.